Scientific Research Publishing

Open Journal of Yangtze Gas and Oil, 2020, 5, 188-199
https://www.scirp.org/journal/ojogas
ISSN Online: 2473-1900
ISSN Print: 2473-1889

Experimental Investigation on Hydrothermal Reduction of Sulfates to H_2S and Organic Sulfides by Ethene

Chao Han[1], Kangle Ding[1,2,3*], Yan Liu[4], Fujia Guan[5], Mei Zou[1], Zhenzhen Yu[1], Yi Wu[1]

[1]Key Laboratory of Exploration Technologies for Oil and Gas Resources, Ministry of Education, Yangtze University, Wuhan Campus, Wuhan, China
[2]Shandong Provincial Key Laboratory of Depositional Mineralization & Sedimentary Mineral, Shandong University of Science and Technology, Qingdao, China
[3]College of Chemistry and Environmental Engineering, Yangtze University, Jingzhou, China
[4]College of Resources and Environment, Yangtze University, Wuhan Campus, Wuhan, China
[5]College of Petroleum Engineering, Yangtze University, Wuhan Campus, Wuhan, China
Email: *dingkl@yangtzeu.edu.cn

How to cite this paper: Han, C., Ding, K.L., Liu, Y., Guan, F.J., Zou, M., Yu, Z.Z. and Wu, Y. (2020) Experimental Investigation on Hydrothermal Reduction of Sulfates to H_2S and Organic Sulfides by Ethene. *Open Journal of Yangtze Gas and Oil*, **5**, 188-199.
https://doi.org/10.4236/ojogas.2020.54015

Received: July 27, 2020
Accepted: September 4, 2020
Published: September 7, 2020

Abstract

The kinetic characteristics of alkenes involved in thermochemical sulfate reduction (TSR) have been never reported in geological literature. In this study, TSR by ethene under hydrothermal conditions was performed in the constrained simulation experiments. Typical TSR products consisted of H_2S, CO_2, mercaptans, sulfides, thiophenes derivatives and benzothiophene. The apparent activation energy E and apparent frequency factor A for TSR by ethene were determined as 76.370 kJ/mol and 4.579 s^{-1}, respectively. The lower activation energy for ethene involved in TSR relative to ethane suggested that the reactivity of ethene is much higher than that of ethane, in accordance with the thermodynamic analysis. Rate constants were determined experimentally using first-order kinetics extrapolate to $MgSO_4$ half-lives of 67.329 years - 3.053 years in deep burial diagenetic settings (120˚C - 180˚C). These values demonstrate that the reaction rate for TSR by ethene is extraordinarily fast in high-temperature gas reservoirs (120˚C - 180˚C). Consequently, the newly formed ethene from thermal cracking and TSR alteration of natural gas and/or petroleum could not survive after TSR process and were rarely detected in natural TSR reservoirs.

Keywords

Thermochemical Sulfate Reduction (TSR), Ethene, Simulation Experiments, Thermodynamic Analysis, First-Order Kinetics

1. Introduction

High sour gas with >10% H_2S (hydrogen sulfide) has been reported in reservoirs from the Upper Permian Changxing Formation and Lower Triassic Feixianguan Formation in the NE Sichuan Basin [1]-[10]. The elevated H_2S (up to 62%) is attributed to thermochemical sulfate reduction (TSR) in deep buried Triassic and Permian reservoirs with vertical depths over 4.8 km [8]. TSR is an organic-inorganic interaction between sulfates and hydrocarbons in high temperature diagenetic settings, in which sulfates are reduced to H_2S, organic sulfides and elemental sulfur (S^0) while hydrocarbons are oxidized to carbon dioxide (CO_2) and water [11]. TSR-derived H_2S not only critically affects the economic proportion of hydrocarbon gas, but is highly toxic to human beings and corrosive for petroleum processing facilities. H_2S gas risk has become one of the major concerns for exploration in deeply buried carbonates [4] [5] [6]. Some laboratory experiments with gaseous saturated hydrocarbons were carried out to investigate the formation mechanism of elevated H_2S in sour gas from TSR zones [12]-[17]. However, up to now, few TSR simulation studies utilized alkenes as reducing agents for sulfates [18]. Although alkenes are absent or only trace components in most natural gas and petroleum, they are produced in appreciable amounts during thermal degradation of kerogen [19] as well as in many previous TSR experiments [12] [18] [20] [21] [22] [23]. Notably, it was reported that alkenes were the most reactive hydrocarbon type during TSR [18], and the rapid increase in the yield of ethanethiol and propanethiol was closely related to the generation of ethylene and propylene from hexadecane thermal cracking at high temperatures [20]. Nevertheless, the kinetics of TSR by alkenes needs further investigation due to no reports related. To fill this gap, a series of simulation experiments on the reactions between magnesium sulfate ($MgSO_4$) and ethene (C_2H_4) were conducted under controlled hydrothermal conditions. C_2H_4 was selected as a representative of intermediate hydrocarbon species during TSR. Anhydrous $MgSO_4$ was utilized as oxidants for hydrocarbons due to its effective oxidant of hydrocarbons without the addition of H_2S [24]. The objectives of the present study are to:

1) Investigate the thermodynamic characteristics of TSR by ethene;
2) Determine the kinetic parameters for sulfate reduction by ethene;
3) Discuss the reason that alkenes were not detected in natural TSR zones.

2. Experiment

$MgSO_4$ is analytical pure, purchased from Aladdin Industrial Corporation (Shanghai, China). C_2H_4 (99.999%) was supplied by Wuhan Newradar Special Gas Co., Ltd.. Simulation experiments on the reduction of $MgSO_4$ by C_2H_4 were operated at elevated temperatures using an autoclave. The autoclave was made of Hastelloy C-276 alloy with a volume of 200 mL. The sample basket is a quartz glass cylinder with a height of 40 mm and diameter of 20 mm. The quartz glass cylinder has a bottom to hold $MgSO_4$ powder and its other side is left open. The

basket was placed on the bottom of the reactor. Each time, the basket with about 2.000 g $MgSO_4$ powder and 1.0 mL distilled water was put into the reactor, and then the reactor was vacuumed. Ethene was charged to a given pressure. In the reaction system of C_2H_4-$MgSO_4$-H_2O, the initial pressure was about 2.5 MPa at room temperature and the final pressure of the reaction system ranged from 4.5 MPa - 5.6 MPa. The reactor was first heated to 250˚C directly and then to the final temperatures by a program control. The final temperatures were 280˚C, 300˚C, 320˚C, 340˚C and 360˚C, and the heating times were 240 h, 400 h, 560 h, 720 h and 880 h, respectively. Constant heating rate β is set as 0.125˚C/h. After simulation experiments, the basket with reaction products was taken out of the autoclave, firstly put into an oven to be heated at 120℃ for about 6 h to remove water, and then heated in a muffle at 500˚C. The weight of solid products was measured by an electron balance. The calculation of TSR conversions was based on gravimetry. The products were characterized by gas chromatography (GC), gas chromatography-mass spectrometry (GC-MS) and X-ray diffractometer (XRD) methods, respectively.

After thermal experiments, headspace gaseous products of the tube reactor were removed through the valve, and characterized using an Agilent 6890 gas chromatograph (Agilent Technologies, Palo Alto, CA, USA). Subsequently, 2 mL of dichloromethane (DCM) was then injected into the reaction vessel through the valve to extract organic products, and then organic sulfur products in the DCM extract were analyzed by gas chromatography-mass spectrometry (GC-MS). The analysis of the extracted organic sulfur products was carried out at Beijing Risun Chemical Technology Institute Co., Ltd., China (courtesy of Shijuan Du). Characteristics of the crystalline structure of the solid products at the termination of each experiment were confirmed by a PANalytical X'Pert PRO X-ray diffractometer (PANalytical Co., Almelo, Netherlands). The analysis of the crystalline structure of the solid products was carried out at Beijing Risun Chemical Technology Institute Co., Ltd., China (courtesy of Xinpo Feng). Detailed operation conditions for GC, GC-MS and XRD are available in Ding *et al.* (2014, 2016) [25] [26].

3. Results and Discussion

3.1. TSR Products

According to the GC analysis, the composition of gaseous products from the reaction between C_2H_4 and $MgSO_4$ was shown in **Table 1**. It was found that gaseous products in the temperature range of 280˚C - 360˚C were composed of CH_4, C_2H_6, C_3H_8, C_3H_6, n-C_4H_{10}, i-C_4H_{10}, H_2S, CO_2, H_2, CH_3SH, C_2H_5SH, CH_3SCH_3 (**Table 1**). Thereinto, C_1~C_4 hydrocarbons and H_2 gas were derived from complex polymerization-decomposition of C_2H_4 and/or alteration of hydrocarbons by TSR at elevated temperatures. H_2S and CO_2 were typical TSR products as had been documented in previous geological observations [3] [8] [11] as well as laboratory simulation experiments [6] [13] [14] [15] [17] [20] [22] [27]. The contents of sour gases increased with increasing temperatures at 280˚C

- 360˚C (Figure 1), which indicated elevated temperatures were favorable for TSR occurring. The reaction pathway for sour gas formation could be written as:

$$SO_4^{2-} + C_2H_4 \rightarrow H_2S + 2CO_2 + H_2O \quad (1)$$

Labile organosulfur compounds (LSC), such as CH_3SH, C_2H_5SH, CH_3SCH_3 (Table 1), were generated from H_2S reacting with hydrocarbons [1] [20]. Figure 2 indicated the contents of ethene and organic sulfides vs. temperature. Figure 2 indicated the contents of ethene and organic sulfides vs. temperature. With the decrease of C_2H_4, contents of LSC vs. temperature exhibited a positive relationship in Figure 2. The diminishing C_2H_4 resulted from TSR effect as well as thermal chemical alteration (Figure 1 and Figure 2).

Table 1. Composition of gaseous products at elevated temperatures (%).

Temperature (˚C)	CH_4	C_2H_6	C_2H_4	C_3H_8	C_3H_6	n-C_4H_{10}	i-C_4H_{10}	H_2S	CO_2	H_2	CH_3SH	C_2H_5SH	CH_3SCH_3
280	10.018	0.171	81.645	0.094	0.069	0.026	0.009	0.223	1.598	4.077	0.156	1.129	0.784
300	11.711	0.241	66.057	0.093	0.237	0.002	0.001	0.925	5.367	4.955	2.349	6.419	1.645
320	14.150	0.185	54.054	0.104	0.083	0.000	0.000	2.123	9.078	5.563	3.374	10.447	0.840
340	17.897	0.157	40.279	0.066	0.034	0.000	0.000	3.660	12.475	3.350	4.843	15.368	1.871
360	24.821	0.183	29.212	0.003	0.000	0.000	0.000	5.031	12.092	3.547	5.007	16.546	3.559

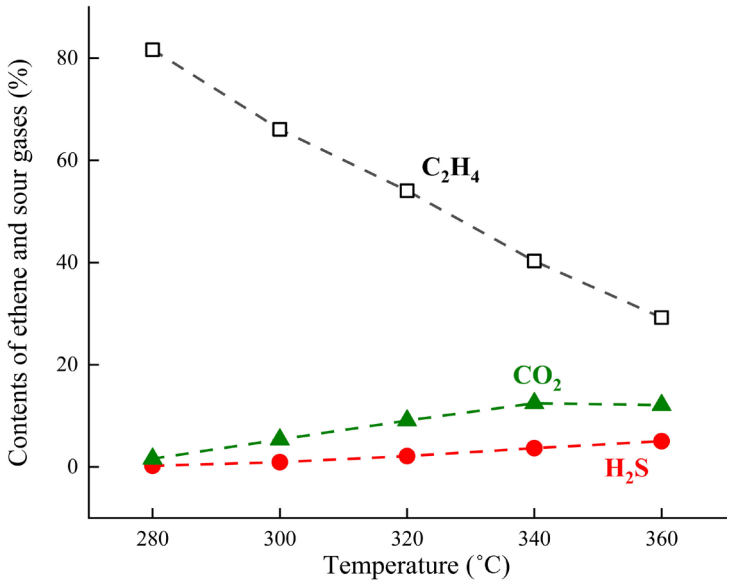

Figure 1. Contents of ethene and sour gases vs. temperature.

The qualitative and quantitative results of sulfur compounds in the DCM extract were listed in Table 2. Besides H_2S and LSC, thiophene derivatives and benzothiophene were also detected in the DCM extract (Table 2). Thiophene derivatives and benzothiophenes are stable organic sulfur compounds (SOSCs) relative to LSC. It can be inferred from Ding *et al.* (2016) [26] that the thermal stability order for mercaptans, sulfides, thiophene derivatives and benzothiophene is benzothiophene > thiophene derivatives > mercaptans or sulfides. Therefore, the

formation of the SOSCs in Table 2 should be attributed to thermal alteration of LSC [22]. The positive correlation between contents of SOSCs and temperature in Figure 3 indicated that the conversion of inorganic sulfur of $MgSO_4$ to thiophene sulfur in TSR was enhanced by elevated temperatures. Tentative formation pathways for LSC and SOSCs in this study were given in Equations (2) and (3):

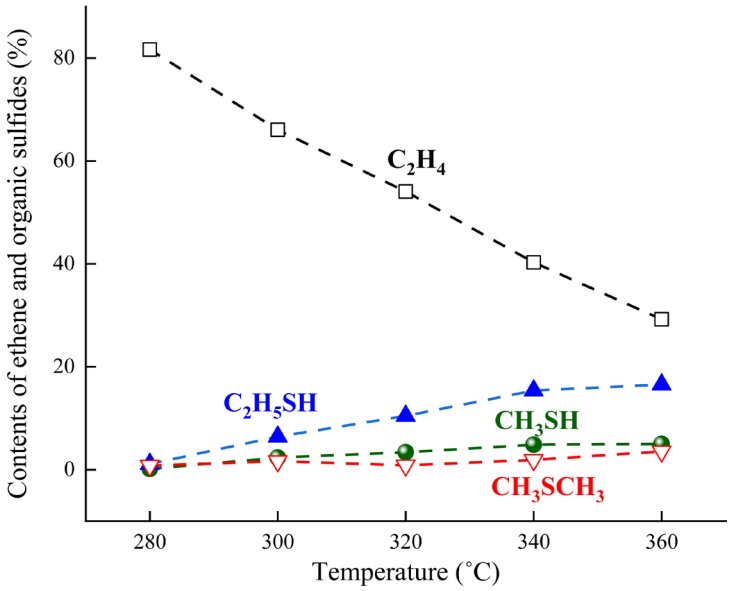

Figure 2. Contents of ethene and organic sulfides vs. temperature.

Table 2. Contents of Table 2 sulfur compounds in the DCM extract (μg·g^{-1}).

Temperature (˚C)	H_2S	CH_3SH	C_2H_5SH	CH_3SCH_3	Thiophene derivatives	Benzothiophene
280	20.801	12.426	355.362	56.693	11.816	0.000
300	17.448	9.790	687.305	78.979	30.441	11.575
320	12.175	36.716	871.844	350.355	48.109	25.573
340	15.022	18.459	899.248	658.624	73.854	40.741
360	11.459	15.535	917.930	311.632	146.430	67.036

$$H_2S + C_2H_4 = C_2H_5SH \quad (2)$$

$$C_2H_5SH \longrightarrow CH_3SH + CH_3SCH_3 + \text{(2-methylthiophene)} + \text{(benzothiophene)} \quad (3)$$

Some black material was observed on the surface of solid products at 360˚C. After calcinations at 500˚C, the solid products turned white. Therefore, the black deposit corresponded to be coke [22]. X-ray powder diffraction patterns of solid reaction products at 360˚C were shown in Figure 4. From the X-ray patterns, two distinct crystallographic phases, MgO and $MgSO_4$ were found to coexist in the products. These results suggested that MgO was produced during TSR by

C_2H_4. Based on the above analysis, it was concluded that H_2S, CO_2 and MgO were the main TSR products. Various organic sulfur compounds such as mercaptans, sulfides, thiophenes derivatives and benzothiophene were mainly derived from H_2S reacting with hydrocarbons as well as thermal chemical alteration of LSC at elevated temperatures.

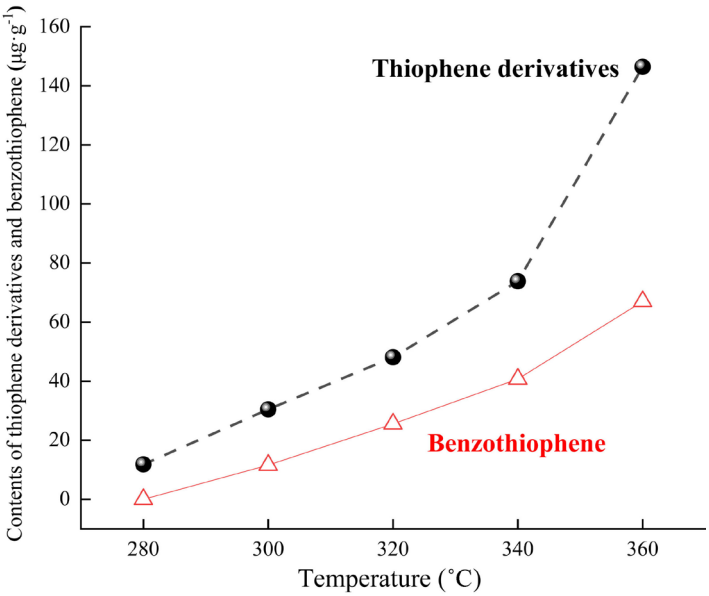

Figure 3. Contents of thiophene derivatives and benzothiophene vs. temperature.

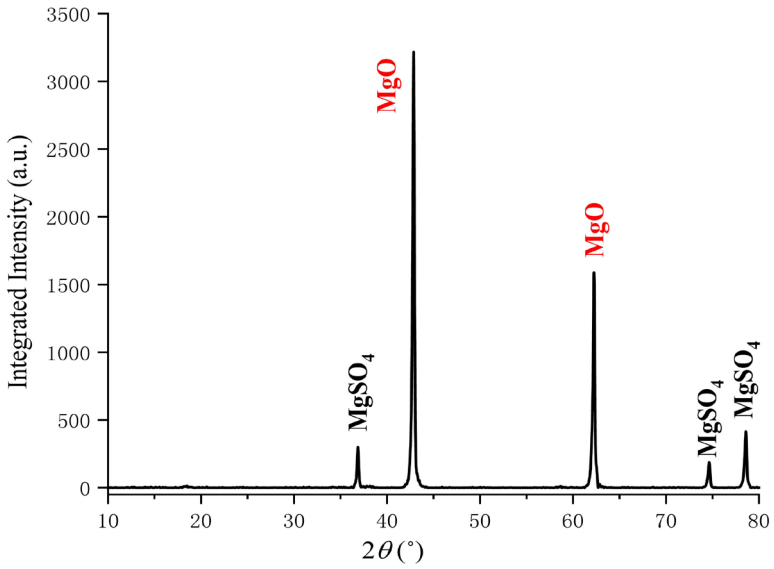

Figure 4. X-ray patterns of the solid products after calcinations.

3.2. Thermodynamic Analysis

Our present experimental results indicated that TSR by ethene could be written as the general Equation (4). Previous study of Ding *et al.* (2011) [15] showed that thermochemical reduction of $MgSO_4$ by ethane (C_2H_6) conformed to Equation (5). Based on Equations (4) and (5), the standard Gibbs free energy of molar

reaction for TSR by ethene or ethane at various temperatures was calculated by use of thermochemical modeling program HSC 6.0 (Outokumpu Research Oy, Pori, Finland) and shown in Figure 5. It is evident that the reactions (4) and (5) proceed spontaneously at 0 - 600˚C according to the negative values of Gibbs free energy (Figure 5). The absolute value of Gibbs free energy of the two reactions increased with increasing temperature, which implied that elevated temperature is favored. Comparing the absolute value of Gibbs free energy of the two reactions (4) and (5) at the same temperature, it can be concluded that ethene thermodynamically more easily participates in TSR than ethane.

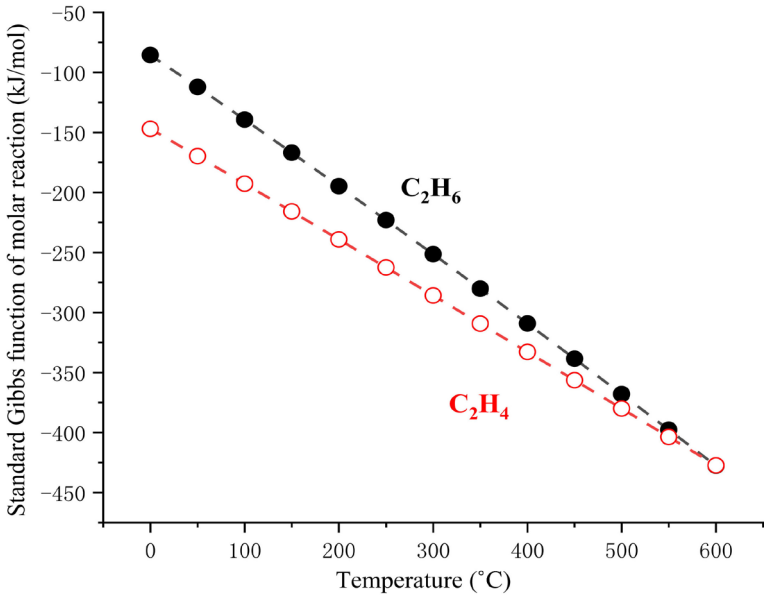

Figure 5. Effect of temperature on standard Gibbs function of TSR by ethene or ethane.

$$C_2H_4 + 1.5MgSO_4 = 1.5MgO + 1.5H_2S + 2CO_2 + 0.5H_2O \quad (4)$$

$$C_2H_6 + 1.75MgSO_4 = 1.75MgO + 1.75H_2S + 2CO_2 + 1.25H_2O \quad (5)$$

3.3. Kinetic Study

In the present study, the molar conversion for the reaction between C_2H_4 and $MgSO_4$ was calculated from the weight change of the solid products and reactants, and the results were given in Figure 6. From Figure 6, it can be seen that TSR conversions increased with increasing temperature. So, temperature is a key factor for TSR by ethene, as had been documented in most previous studies [6] [12] [14] [15] [20] [21] [22] [23].

The reaction of C_2H_4 and $MgSO_4$ is assumed as first order reaction, and its kinetic equation could be written as [28]:

$$\frac{\beta dx}{1-x} = A e^{-E/RT} dT \quad (6)$$

where constant heating rate $\beta = \frac{dT}{dt}$, x is reaction conversion, A is the apparent

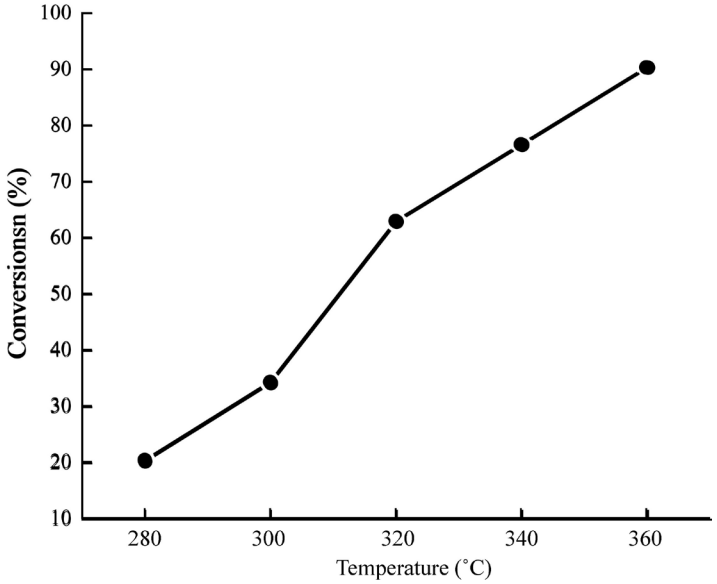

Figure 6. Reaction conversions of $MgSO_4$ vs. temperatures.

frequency factor, E is apparent activation energy, T is absolute temperature and R is the gas constant. According to the study of Ding *et al.* (2008b) [14], the approximate integration of Equation (1) will give

$$-\ln\left[\frac{-\ln(1-x)}{T^2}\right]=\frac{E}{RT}-\ln\frac{AR}{\beta E}\left(1-\frac{2RT}{E}\right) \tag{7}$$

According to the slope and intercept of regressed line in **Figure 7**, the apparent activation energy E and apparent frequency factor A for TSR by ethene were determined as 76.370 kJ/mol and 4.579 s^{-1}, respectively. Notably, Xia *et al.* (2014) [29] reported that the activation energy for reduction of $MgSO_4$ by ethane is 264.5 kJ/mol. The lower activation energy for ethene involved in TSR relative

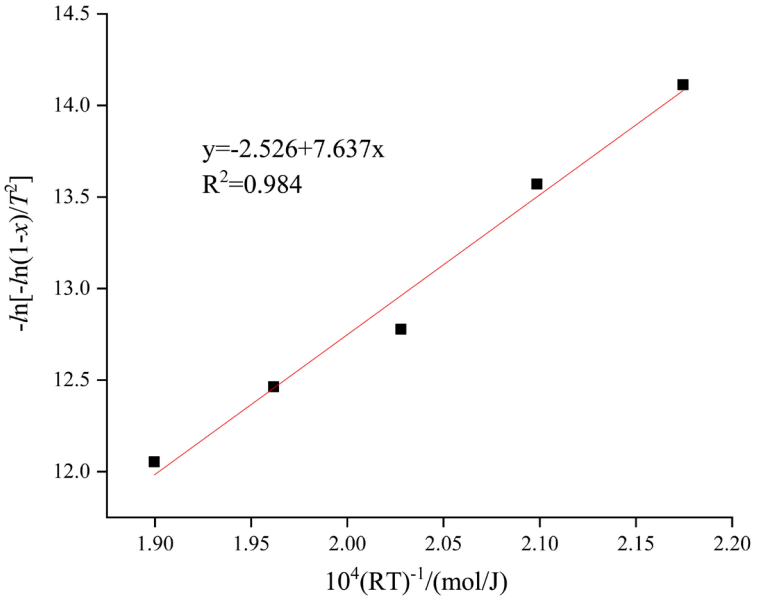

Figure 7. The kinetic regression line for the TSR by ethene.

to ethane suggested that the reactivity of ethene is much higher than that of ethane, in accordance with the above thermodynamic analysis. High reactivity of alkenes is possibly due to their susceptibility to electrophilic attack [6]. The reaction rate constant k and half-live $t_{1/2}$ for TSR by ethene at geological temperatures was determined using Equation (6). The results were listed in Table 3.

Table 3. The reaction rate constants and half-lives for the reduction of $MgSO_4$ by ethene at geological temperatures.

Temperature (˚C)	k (sec^{-1})	$t_{1/2}$ (year)
20	1.128×10^{-13}	1.948×10^{5}
40	8.348×10^{-13}	2.633×10^{4}
60	4.857×10^{-12}	4.526×10^{3}
80	2.315×10^{-11}	949.546
100	9.332×10^{-11}	235.537
120	3.264×10^{-10}	67.329
140	1.012×10^{-09}	21.727
160	2.824×10^{-09}	7.783
180	7.200×10^{-09}	3.053
200	1.696×10^{-8}	1.296
220	3.727×10^{-8}	0.590

Rate constants determined experimentally using first-order kinetics extrapolate to $MgSO_4$ half-lives of 1. 948E+05 years −67.329 years at 20˚C - 120˚C, 67.329 years −7.783 years at 120˚C - 160˚C and 7.783 years −0.590 years at 160˚C - 220˚C. These values demonstrated that the reaction rate for TSR by ethene is very fast in high-temperature gas reservoirs (120˚C - 220˚C). The new formed ethene from thermal cracking of natural gas and/or petroleum could not survive after TSR process. Therefore, alkenes were rarely detected in natural TSR reservoirs. Although the present results of the simulation experiments could not yet be directly applied to the oil & gas exploration in TSR zones, they are theoretically significant for further understanding of the formation mechanisms of thiols in the Triassic Wolonghe gas field as well as elevated thiophene concentrations in the Jurassic reservoirs from the Sichuan Basin, China [1].

4. Conclusion

Thermal reduction of sulfates by alkenes may have implications for origin of OSCs in deep buried geologic settings. In the present study, TSR by ethene was demonstrated under laboratory experimental conditions. The threshold temperature for reduction of $MgSO_4$ by ethene was determined as low as 280˚C, with H_2S, CO_2 and a series of OSCs as the main TSR products. The reactions between ethene and $MgSO_4$ can proceed spontaneously at 0 - 600˚C. Ethene thermodynamically more easily participates in TSR than ethane. The lower activation energy of 76.370 kJ/mol for ethene involved in TSR relative to ethane

suggested that the reactivity of ethene is much higher than that of ethane. The reaction rate for TSR by ethene is very fast in high-temperature gas reservoirs (120˚C - 180˚C), indicating the newly formed ethene from thermal cracking of natural gas and/or petroleum could not survive after TSR process. Therefore, alkenes were rarely detected in natural TSR reservoirs. The present results of the simulation experiments are theoretically significant for further understanding of the formation mechanisms of thiols in the Triassic Wolonghe gas field as well as elevated thiophene concentrations in the Jurassic reservoirs from the Sichuan Basin, China.

Acknowledgements

We gratefully acknowledge financial support by the National Natural Science Foundation of China (No. 41472095), the Open Fund of Key Laboratory of Exploration, Technologies for Oil and Gas Resources (Yangtze University), Ministry of Education (No. K2018-05) and the Foundation of Shandong Provincial Key Laboratory of Depositional Mineralization and Sedimentary Minerals, Shandong University of Science and Technology (Grant No. DMSM2018041).

Conflicts of Interest

The authors declare no conflicts of interest regarding the publication of this paper.

References

[1] Cai, C.F., Worden, R.H., Bottrell, S.H., Wang, L.S. and Yang, C.C. (2003) Thermochemical Sulphate Reduction and the Generation of Hydrogen Sulphide and Thiols (Mercaptans) in Triassic Carbonate Reservoirs from the Sichuan Basin, China. *Chemical Geology*, **202**, 39-57. https://doi.org/10.1016/S0009-2541(03)00209-2

[2] Cai, C.F., Xie, Z.Y., Worden, R.H., Hu, G.Y., Wang, L.S. and He, H. (2004) Methane-Dominated Thermochemical Sulphate Reduction in the Triassic Feixianguan Formation East Sichuan Basin, China: Towards Prediction of Fatal H_2S Concentrations. *Marine and Petroleum Geology*, **21**, 1265-1279. https://doi.org/10.1016/j.marpetgeo.2004.09.003

[3] Cai, C.F., Zhang, C.M., He, H. and Tang, Y.J. (2013) Carbon Isotope Fractionation during Methane Dominated TSR in East Sichuan Basin Gas Fields, China: A Review. *Marine and Petroleum Geology*, **48**, 100-110. https://doi.org/10.1016/j.marpetgeo.2013.08.006

[4] Zhu, G.Y., Zhang, S.C., Liang, Y.B., Dai, J.X. and Li, J. (2005) Isotopic Evidence of TSR Origin for Natural Gas Bearing High H_2S Contents within the Feixianguan Formation of the Northeastern Sichuan Basin, Southwestern China. *Science in China Series D Earth Sciences*, **48**, 1960-1971. https://doi.org/10.1360/082004-147

[5] Zhu, G.Y., Zhang, S.C., Liang, Y.B., Ma, Y.S., Guo, T.L. and Zhou, G.Y. (2006) Distribution of High H_2S-Bearing Natural Gas and Evidence of TSR Origin in the Sichuan Basin. *Acta Geologica Sinica*, **80**, 1208-1218. (in Chinese)

[6] Zhang, T., Ellis, G.S., Wang, K., Walters, C.C., Kelemen, S.R., Gillaizeau, B. and Tang, Y. (2007) Effect of Hydrocarbon Type on Thermochemical Sulfate Reduction. *Organic Geochemistry*, **38**, 897-910.

https://doi.org/10.1016/j.orggeochem.2007.02.004

[7] Hao, F., Guo, T.L., Zhu, Y.M., Cai, X.Y., Zou, H.Y. and Li, P.P. (2008) Evidence for Multiple Stages of Oil Cracking and Thermochemical Sulfate Reduction in the Puguang Gas Field, Sichuan Basin, China. *AAPG Bulletin*, **92**, 611-637.

[8] Liu, Q.Y., Worden, R.H., Jin, Z.J., Liu, W.H., Li, J., Gao, B., *et al.* (2013) TSR versus Non-TSR Processes and Their Impact on Gas Geochemistry and Carbon Stable Isotopes in Carboniferous, Permian and Lower Triassic Marine Carbonate Gas Reservoirs in the Eastern Sichuan Basin, China. *Geochimica et Cosmochimica Acta*, **100**, 96-115. https://doi.org/10.1016/j.gca.2012.09.039

[9] Li, K.K., George, S.C., Cai, C.F., Gong, S., Sestak, S., Armand, S., *et al.* (2019) Fluid Inclusion and Stable Isotopic Studies of Thermochemical Sulfate Reduction: Upper Permian and Lower Triassic Gasfields, Northeast Sichuan Basin, China. *Geochimica et Cosmochimica Acta*, **246**, 86-108. https://doi.org/10.1016/j.gca.2018.11.032

[10] Wu, X.Q., Liu, Q.Y., Liu, G.X. and Ni, C.H. (2019) Genetic Types of Natural Gas and Gas-Source Correlation in Different Strata of the Yuanba Gas Field, Sichuan Basin, SW China. *Journal of Asian Earth Sciences*, **181**, Article ID: 103906. https://doi.org/10.1016/j.jseaes.2019.103906

[11] Machel, H. (2001) Bacterial and Thermochemical Sulfate Reduction in Diagenetic Settings—Old and New Insights. *Sedimentary Geology*, **140**, 143-175. https://doi.org/10.1016/S0037-0738(00)00176-7

[12] Yue, C.T., Li, S.Y., Ding, K.L. and Zhong, N.N. (2006) Thermodynamics and Kinetics of Reactions between C_1-C_3 Hydrocarbons and Calcium Sulfate in Deep Carbonate Reservoirs. *Geochemical Journal*, **40**, 87-94.

[13] Pan, C.C., Yu, L.P., Liu, J.Z. and Fu, J.M. (2006) Chemical and Carbon Isotopic Fractionations of Gaseous Hydrocarbons during Abiogenic Oxidation. *Earth and Planetary Science Letters*, **246**, 70-89. https://doi.org/10.1016/j.epsl.2006.04.013

[14] Ding, K.L., Li, S.Y., Yue, C.T. and Zhong, N.N. (2008) Simulation Experiments on the Reaction System of CH_4-$MgSO_4$-H_2O. *Chinese Science Bulletin*, **53**, 1071-1078. https://doi.org/10.1007/s11434-008-0073-3

[15] Ding, K.L., Wang, S.S., Li, S.Y. and Yue, C.T. (2011) Thermochemical Reduction of Magnesium Sulfate by Natural Gas: Insights from an Experimental Study. *Geochemical Journal*, **45**, 97-108. https://doi.org/10.2343/geochemj.1.0103

[16] Truche, L., Bazarkina, E.F., Barré, G., Thomassot, E., Berger, G., Dubessy, J. and Robert, P. (2014) The Role of S_3^- Ion in Thermochemical Sulphate Reduction: Geological and Geochemical Implications. *Earth and Planetary Science Letters*, **396**, 190-200. https://doi.org/10.1016/j.epsl.2014.04.018

[17] He, K., Zhang, S., Mi, J., Ma, Q., Tang, Y. and Fang, Y. (2019) Experimental and Theoretical Studies on Kinetics for Thermochemical Sulfate Reduction of Oil, C_{2-5} and Methane. *Journal of Analytical and Applied Pyrolysis*, **139**, 59-72. https://doi.org/10.1016/j.jaap.2019.01.011

[18] Zhang, S.C., Zhu, G.Y., Chen, J.P. and Liang, Y.B. (2007) A Discussion on Gas Sources of the Feixianguan Formation H_2S-Rich Giant Gas Fields in the Northeastern Sichuan Basin. *Chinese Science Bulletin*, **52**, 113-124. https://doi.org/10.1007/s11434-007-6014-8

[19] González-Vila, F.J., Amblès, A., Del Río, J.C. and Grasset, L. (2001) Characterisation and Differentiation of Kerogens by Pyrolytic and Chemical Degradation Techniques. *Journal of Analytical and Applied Pyrolysis*, **58-59**, 315-328. https://doi.org/10.1016/S0165-2370(00)00196-0

[20] Zhang, T., Ellis, G.S., Walters, C.C., Kelemen, S.R., Wang, K. and Tang, Y. (2008)

Geochemical Signatures of Thermochemical Sulfate Reduction in Controlled Hydrous Pyrolysis Experiments. *Organic Geochemistry*, **39**, 308-328. https://doi.org/10.1016/j.orggeochem.2007.12.007

[21] Zhang T.W., Amrani A., Ellis G.S., Ma, Q.S. and Tang, Y.C. (2008) Experimental Investigation on Thermochemical Sulfate Reduction by H_2S Initiation. *Geochimica et Cosmochimica Acta*, **72**, 3518-3530. https://doi.org/10.1016/j.gca.2008.04.036

[22] Ding, K.L., Li, S.Y., Yue, C.T. and Zhong, N.N. (2008) A Simulation on the Formation of Organic Sulfur Compounds in Petroleum from Thermochemical Sulfate Reduction. *Journal of Fuel Chemistry and Technology*, **36**, 48-54. https://doi.org/10.1016/S1872-5813(08)60011-0

[23] Zhao, H., Liu, W., Borjigin, T., Zhang, J. and Wang, X. (2019) Study of Thermochemical Sulfate Reduction of Different Organic Matter: Insight from Systematic TSR Simulation Experiments. *Marine and Petroleum Geology*, **100**, 434-446. https://doi.org/10.1016/j.marpetgeo.2018.11.009

[24] Gillaizeau, B. and Tang, Y. (2001) Reaction Mechanistic Studies for the Thermochemical Sulfate Reduction. 20*th International Meeting on Organic Geochemistry*, Nancy, 10-14 September 2001, Abstract.

[25] Ding, K.L., Wang, S.S. and Gao, D.W. (2014) Kinetics of N-S Atom Exchange in the Pyrrole-H_2S System. *Arabian Journal for Science and Engineering*, **39**, 5537-5541. Https://Doi.Org/10.1007/S13369-014-1112-9

[26] Ding, K.L., Mei, P. and Luo, Y. (2016) Pyrite-hydrocarbon Interaction under Hydrothermal Conditions: An Alternative Origin of H_2S and Organic Sulfur Compounds in Sedimentary Environments. *Acta Geologica Sinica—English Edition*, **90**, 2133-2148. https://doi.org/10.1111/1755-6724.13027

[27] Zhang, S.C., Shuai, Y.H. and Zhu, G.Y. (2008) TSR Promotes the Formation of Oil-Cracking Gases: Evidence from Simulation Experiments. *Science in China Series D*: *Earth Sciences*, **51**, 451-455. https://doi.org/10.1007/s11430-008-0009-4

[28] Fu, J.M. and Qin, K.Z. (1995) Kerogen Geochemistry. Guangdong Science & Technology Press, Guangzhou, 544-547.

[29] Xia, X.Y., Ellis, G.S., Ma, Q.S. and Tang, Y.C. (2014) Compositional and Stable Carbon Isotopic Fractionation during Non-Autocatalytic Thermochemical Sulfate Reduction by Gaseous Hydrocarbons. *Geochimica et Cosmochimica Acta*, **139**, 472-486. https://doi.org/10.1016/j.gca.2014.05.004